Progress In Electromagnetics Research Letters, Vol. 65, 49–55, 2017

Wideband Balanced Filters with Wideband Common Mode Suppression Using Coupled Lines

Kuan Deng* **and Zhengyu Chen**

Abstract—A novel balanced filter circuit with wideband common mode suppression using coupled lines is proposed in this paper. A wideband filter with half open stubs is used to realize two transmission zeros for the differential mode passband. The common mode can be suppressed over 15 dB from 0 GHz to $3f_0$ (f_0 is the center frequency of the passband) with insertion loss greater than 15 dB over the upper stopband. A balanced filter with 3-dB fractional bandwidths of 38% is designed and fabricated. Good agreement can be observed between measured results and theoretical expectations.

1. INTRODUCTION

Compared with single-ended circuits, balanced circuits have advantages of higher immunity to the environmental noises, better dynamic range, and lower electromagnetic interference (EMI), which are imperatively needed in communication systems [1, 2]. In the past few years, many microstrip balanced filters for single-band, dual-band and wideband with common mode suppression have been realized [3–15]. In [5, 6], branch-line couplers are cascaded to realize a wide passband for the differential mode; however, out-of-band common mode suppression cannot be solved. Broadside coupled microstrip-slot-microstrip structures can also be utilized to realize an ultra-wideband (UWB) differential filter in [7–10], but the transmission zeros near the differential mode passband are difficult to increase. Some ultra-wideband (UWB) balanced bandpass filters based on double-sided parallel-strip lines (DSPSLs) are introduced in [11, 12], but the upper stopband for the differential mode should be further extended. Several wideband balanced filters with high selectivity for the differential mode passband are introduced in our former works [13, 14], but the common mode suppression level is not so good. Compact wideband balanced filters using wire-bonded multiple conductor transmission lines are also shown in [15], but the selectivity for the differential mode passband is not so ideal due to lack of transmission zeros.

In this paper, a wideband balanced filter based on common coupled lines with wideband common mode suppression is proposed. Two transmission zeros for the differential mode passband can be easily realized without complex coupling circuits, and several transmission zeros can be used to realize wideband common mode suppression, due to the all-stop transmission characteristic of the coupled lines. Fig. 1 shows two conventional two-stage open coupled filter circuits with two open/shorted loaded stubs (θ, Z_1) connected in the end of two input/output coupled lines (Z_{e1}, Z_{o1}, θ). The simulated results of Fig. 1 are shown in Figs. 2(a)–(b). As shown in Fig. 2(a), the out-of-band suppression and selectivity of the filter can be further improved due to the two shorted loaded stubs (Z_1). In addition, for the simulated results in Fig. 2(b), an all-stop transmission characteristic can be realized by one/two open stubs, and the stopband level of one open and one shorted subs is better than the two open stubs. Therefore, when the coupled circuits of Fig. 1 are used to design balanced filters, the symmetrical shorted stubs can be used to design a high selectivity passband for the differential mode, and the asymmetrical open/shorted stubs can be used to suppress common mode over a wide band, and the asymmetrical circuit model

Received 12 November 2016, Accepted 9 December 2016, Scheduled 9 January 2017
* Corresponding author: Kuan Deng (kuandengchina@163.com).
The authors are with the School of Electronics and Information Engineering, Jinling Institute of Technology, Nanjing 211169, China.

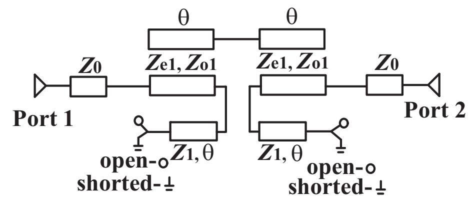

Figure 1. Improved coupled line filter circuits with open/shorted loaded stubs.

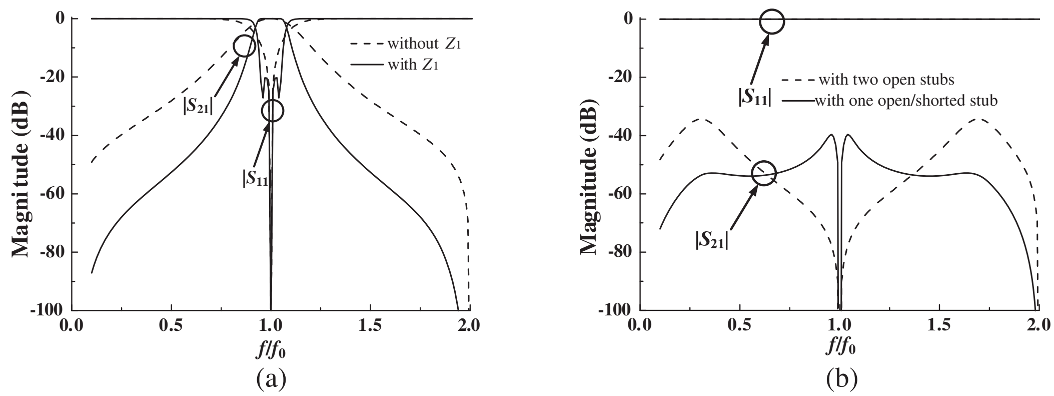

Figure 2. Simulated results of Fig. 1. (a) With/without shorted stubs Z_1, (b) results with one/two open stubs. ($Z_1 = 40\,\Omega$, $Z_{e1} = 160\,\Omega$, $Z_{o1} = 100\,\Omega$, $Z_0 = 50\,\Omega$).

can have more freedom to design different balanced circuits, which are different from former balanced circuits in [3–15]. Moreover, some other stubs can also be considered to increase the passband order and transmission zeros for the differential mode [16], and the increased transmission zeros can be used to further improve the common mode suppression. For further demonstration, detailed theoretical design for the balanced filter will be given next.

2. ANALYSIS AND DESIGN OF PROPOSED BALANCED FILTER

Figure 3(a) shows an ideal circuit of the balanced filter structure with half-wavelength stubs. Four half-wavelength open stubs are shunted connected in input/output ports 1, 1′, 2, 2′. Two open coupled lines (Z_{e1}, Z_{o1}, θ) with shorted loaded stubs (Z_1, θ) are located in the middle of the balanced filter circuit, and four microstrip lines with characteristic impedance $Z_0 = 50\,\Omega$ are connected to ports 1, 1′ and ports 2, 2′.

When the differential mode signals are excited from ports 1 and 1′ in Fig. 3(a), a virtual short appears along the symmetric line, and the centre coupling structure for the input coupled line is a shorted stub with characteristic impedance Z_1 and electrical length θ, as shown in Fig. 3(b). The *ABCD* matrices of the differential mode circuit can be defined as $M_1 \times M_{block1} \times M_{block2} \times M_1$, and M_1 (half-wavelength stubs), M_{block1}, M_{block2} can be obtained from [16]. After *ABCD*- and *Y*-parameter conversions, when $S_{dd21} = 0$, the transmission zeros of the differential mode are obtained as

$$\theta tz1 = \pi/4, \quad \theta tz2 = 3\pi/4 \tag{1}$$

In addition, the transmission poles in the passband can be calculated when $S_{dd11} = 0$. A third-order equation for θ versus Z_1, Z_2, Z_{e1} and Z_{o1} can be obtained for this case. When Z_0 is fixed, three roots for $S_{dd11} = 0$ can be found by properly choosing the relationships of Z_1, Z_2, Z_{e1} and Z_{o1}, and then three transmission poles in the passband can be achieved. In addition, the external quality factor Q_e of the parallel-coupled line can be given by [14]:

$$Qe = 2\pi Z_0^2/(Z_{e1} - Z_{o1})^2 \tag{2}$$

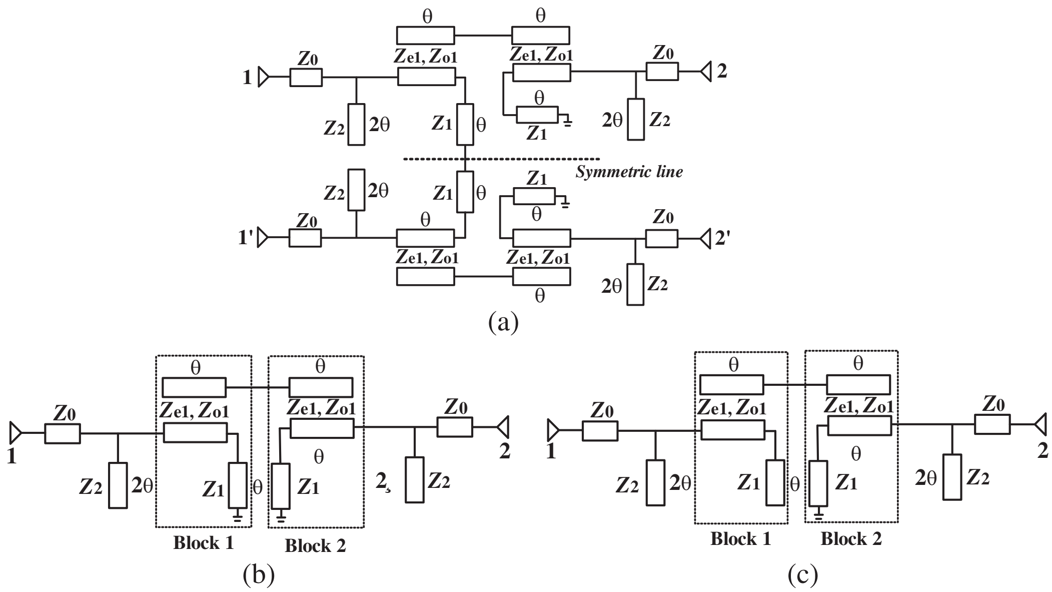

Figure 3. (a) The ideal circuit of the balanced filter, (b) differential mode circuit, (c) common mode circuit.

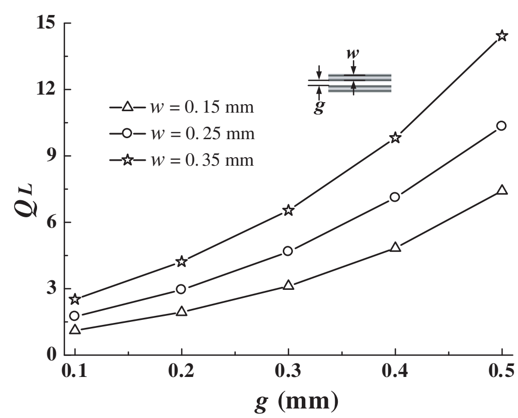

Figure 4. Simulated Q_L for parallel-coupled line versus gap size g.

Once Z_{e1} and Z_{o1} of the parallel-coupled line are known, the line width w and gap g can be simulated from Ansoft Designer v3.0.

In addition, the loaded quality factor Q_L and 3-dB bandwidth $\triangle f$ of the parallel-coupled line are related by

$$Q_L = f_0/\Delta f \quad (3)$$

The simulated Q_L versus gap g for different line widths is shown in Fig. 4. For a lossless case, when $Q_L = Q_e$, and f_0 and $\triangle f$ are specified, Z_{e1} and Z_{o1} of the parallel-coupled line can be determined, and the parameters of the parallel-coupled line can be obtained. For example, when $f_0 = 1.0\,\text{GHz}$ and $\triangle f = 0.3\,\text{GHz}$, and gap $g = 0.26\,\text{mm}$ ($\varepsilon_r = 2.65$, $h = 0.5\,\text{mm}$) can be obtained for the case of $Q_L = Q_e \approx 3.3$. From Eq. (2), we can obtain Z_{e1} and Z_{o1} ($Z_{e1} = 154\,\Omega$, $Z_{o1} = 85.1\,\Omega$), and then the line width w can be determined ($w = 0.2\,\text{mm}$).

The simulated frequency responses of Fig. 3(b) are shown in Fig. 5. Due to the introduced two half-wavelength open stubs, two transmission zeros (f_{tz1}, f_{tz2}) are produced near the passband for the differential mode, and the three in-band transmission poles reflect the fact that $S_{dd11} = 0$ has three real solutions when Z_1, Z_2, Z_{e1} and Z_{o1} are properly selected. For a high selectivity balanced filter,

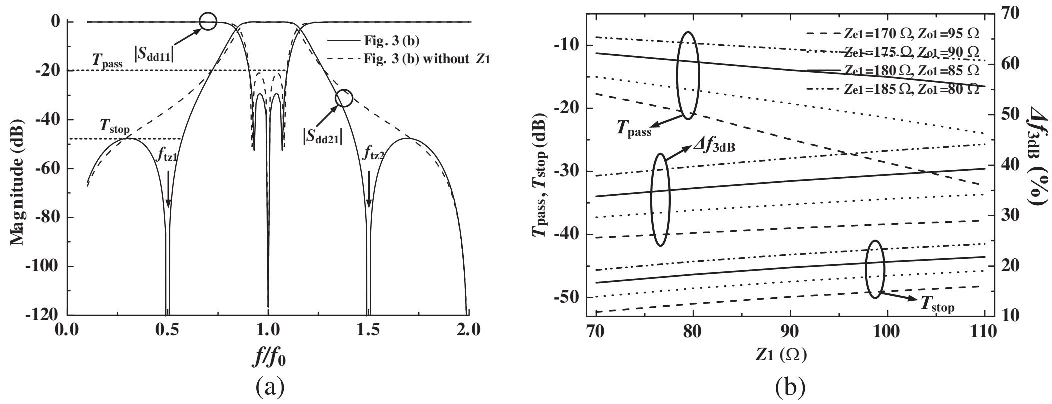

Figure 5. Simulated frequency responses of Fig. 3(b). (a) $|S_{dd21}|$ & $|S_{dd11}|$ ($Z_1 = 100\,\Omega$, $Z_2 = 100\,\Omega$, $Z_{e1} = 170\,\Omega$, $Z_{oo} = 85\,\Omega$), (b) 3-dB bandwidth, T_{stop}, T_{pass} versus Z_1, Fig. 3(b).

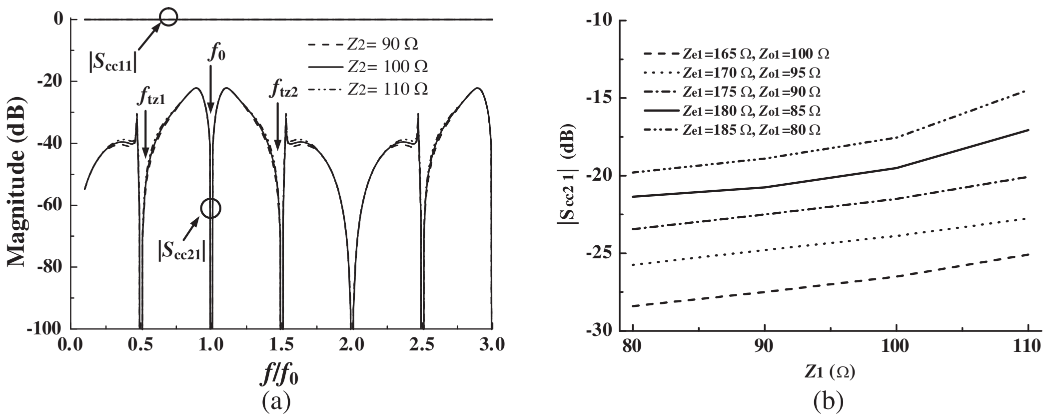

Figure 6. Simulated frequency responses of Fig. 3(c). (a) Versus Z_1, $Z_1 = 120\,\Omega$, $Z_{e1} = 170\,\Omega$, $Z_{o1} = 100\,\Omega$, (b) $|S_{cc21}|$ versus Z_{e1}, Z_{o1}, Z_2, $Z_0 = 50\,\Omega$, $Z_2 = 100\,\Omega$.

the concerned filter characteristics mainly include the 3-dB bandwidth, maximal $|S_{21}|$ (T_{stop}, dB) in the stopband and maximal in-band $|S_{11}|$ (T_{pass}, dB) referring to the responses in Fig. 5(a), and Fig. 5(b) shows the concerned filter characteristics versus the shorted loaded stub Z_2, Z_{e1}, Z_{o1}. The 3-dB bandwidth and T_{stop} increase as Z_1 increases; T_{pass} decreases as Z_1 increases. In this way, the in-band and out-of-band performances of the differential mode can be further improved by optimizing the characteristic impedance value of the shorted stubs (Z_2), when Q_L, Q_e of the parallel-coupled lines are chosen.

When the common mode signals are excited from ports 1 and 1′, a virtual open appears along the symmetric line in Fig. 3(c), and the left side of the balanced filter is an open loaded stub with characteristic impedance Z_2 and electrical length θ. As discussed for the differential mode, the matrices of the common mode circuit can also be defined as $M_1 \times M_{block1} \times M_{block2} \times M_1$, and M_1 and M_{block2} are similar to the differential mode circuit. The structure of M_{block1} is open coupled lines loaded with an open stub, and the the $ABCD$ matrix of M_{block1} is different from the differential mode circuit. When $S_{cc21} = 0$, three transmission zeros can be obtained as f_{tz1}, f_0, f_{tz2}, and the transmission zero located at f_0 is introduced by the open loaded stub (Z_2, θ). The other transmission zeros f_{tz1}, f_{tz2} are similar to the differential mode circuit.

Figure 6 shows the simulated frequency responses of the common mode for Fig. 3(c). Obviously, broadband common mode suppression can be easily achieved with the decrease of characteristic impedance Z_1 and the coupling coefficient of the parallel-coupled line. In addition, the locations of the three transmission zeros f_{tz1}, f_0, f_{tz2} do not change with the characteristic impedances Z_1, Z_2, Z_{e1},

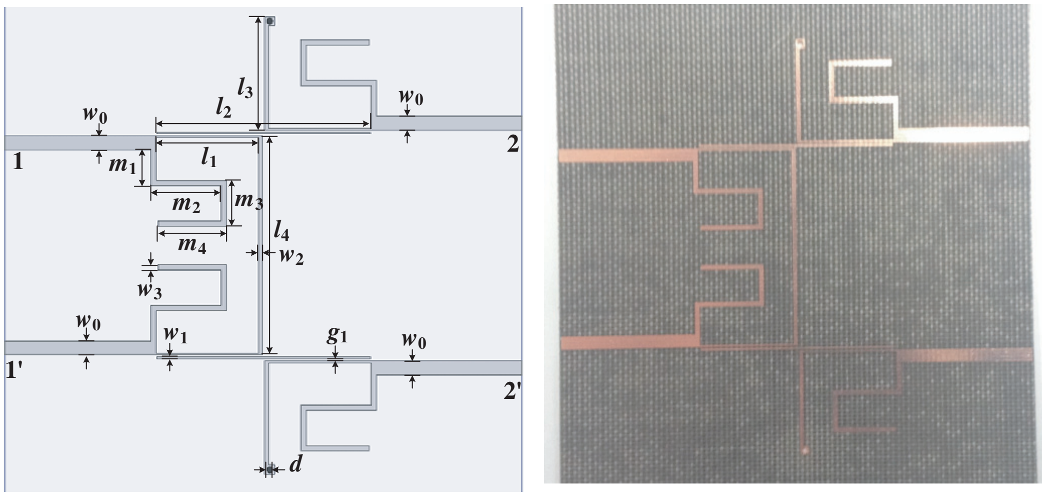

(a) (b)

Figure 7. Geometry and photograph of the proposed balanced filter. (a) Geometry, (b) photograph.

Table 1. Parameters of the proposed balanced filter. (ε_r =2.65, h = 0.5 mm, and $\tan\delta$ = 0.003, $f_0 = 5.0$ GHz).

	Circuit parameters (Ω)	Structure parameters (mm)
Proposed balanced filter	$Z_1 = 100$, $Z_2 = 90$ $Z_{e1} = 171$, $Z_{o1} = 88$ $1.5\lambda_0 \times 1.0\lambda_0$	$l_1 = 10.2$, $l_2 = 21.2$, $l_3 = 11.18$, $l_4 = 21.56$, $m_1 = 3.5$, $m_2 = 7.0$, $m_3 = 4.5$, $m_4 = 6.8$, $w_0 = 1.37$, $w_1 = 0.18$, $w_2 = 0.4$, $w_3 = 0.5$, $d = 0.6$, $g_1 = 0.2$

Z_{o1}, and the wide common mode suppression from 0 to $3f_0$ can be easily realized.

Referring to the discussions and simulated results, the 3-dB bandwidth of the balanced filter is chosen as 36%, and the final parameters (Fig. 7) for the balanced filter are listed in Table 1. Fig. 8 illustrates the simulated results of the balanced filter. For the balanced filter, two simulated transmission zeros are located at 2.5, and 7.5 GHz, and the in-band insertion loss is less than 0.5 dB with 3-dB bandwidth approximately 37.6% (4.02–5.9 GHz); for the common mode, the insertion loss is greater than 15 dB from 0 GHz to 14.1 GHz ($2.82f_0$).

3. MEASURED RESULTS AND DISCUSSIONS

A photograph is shown in Fig. 7, and the measured results of the balanced filter are illustrated in Fig. 8. As shown in Fig. 8(a), for differential mode, the 3-dB bandwidth is 38% (4.06–5.96 GHz) with return loss greater than 15 dB (4.17–5.76 GHz), and three measured transmission zeros are located at 2.62, 6.89 GHz. Over 15-dB upper stopband is realized from 6.38 to 14.1 GHz ($2.82f_0$), and the passband group delay is less than 2.0 ns. For the common mode of Fig. 8(b), over 15-dB common mode suppression is achieved from 0 GHz to 14.8 GHz ($2.96f_0$).

Table 2 illustrates the comparisons of measured results for different balanced filters. Compared with other balanced filters [3–15], the balanced filter can keep the wideband common mode suppression, and more transmission zeros close to the differential mode passband can be achieved to improve skirt selectivity. Moreover, to further extend the bandwidth of the balanced filter, patterned ground-plane technology [7] can be introduced to the balanced bandpass filter. Some bandstop networks can also be considered to extend the upper stopband for the differential mode passband [16].

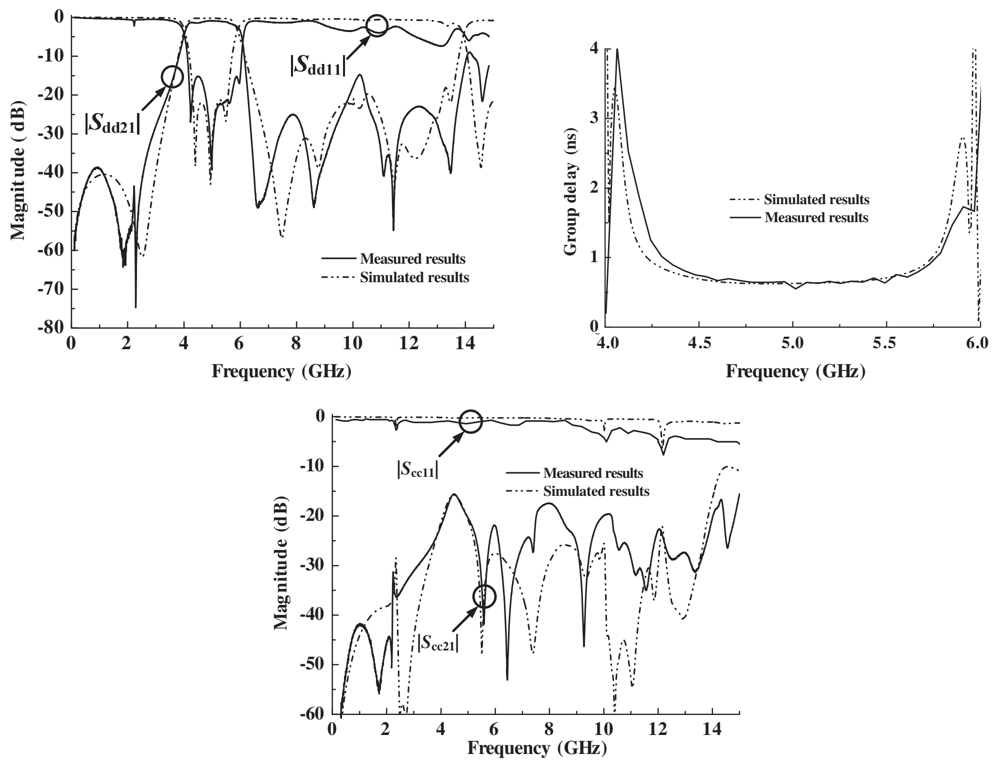

Figure 8. Measured and simulated results of the balanced filter. (a) Differential mode and group delay, (b) common mode.

Table 2. Comparisons of measured results for some wideband balanced filters.

Filter Structures	Transmission zeros, (f_0)	3-dB bandwidth $\|S_{dd21}\|$	Upper stopband $\|S_{dd21}\|$, dB	$\|S_{cc21}\|$, dB
Ref. [3]-I	3 (1.0 GHz)	10.5%	< -30, $2.9f_0$	< -30, (0–2.7)
Ref. [4]-I	2 (1.57 GHz)	11%	< -20, $2.5f_0$	< -20, (0–3.3)
Ref. [5]	0 (4.0 GHz)	62.5%	< -20, $2.3f_0$	< -20, (2.7–5.8)
Ref. [6]	2 (1.0 GHz)	119%	< -15, $2.1f_0$	< -12, (2.6–12.0)
Ref. [7]	2 (6.8 GHz)	120%	< -15, $2.6f_0$	< -17, (0–14.2)
Ref. [8]	0 (3.8 GHz)	105%	< -15, $2.3f_0$	< -30, (0–8.0)
Ref. [9]	2 (6.8 GHz)	115%	< -20, $2.2f_0$	< -20, (0–14.0)
Ref. [10]	2 (4.0 GHz)	115%	< -20, $2.2f_0$	< -20, (0–10.0)
Ref. [11]	1 (3.0 GHz)	110%	< -15, $2.3f_0$	< -20, (0–8.0)
Ref. [12]-I	2 (6.8 GHz)	94%	< -15, $2.3f_0$	< -10, (4.5–8.0)
Ref. [13]	2 (3.0 GHz)	79%	< -25, $2.6f_0$	< -13, (0–8.0)
Ref. [14]-II	2 (6.8 GHz)	70%	< -20, $2.8f_0$	< -14, (0–19.0)
Ref. [15]-II	0 (3.5 GHz)	97%	< -20, $2.4f_0$	< -20, (0–7.5)
This work	**2 (5.0 GHz)**	**38%**	< -15, $2.8f_0$	< -15, **0–14.8**

4. CONCLUSION

In this paper, a wideband high selectivity balanced filter with wideband common mode suppression using coupled lines is proposed. Two transmission zeros close to the differential mode passband can be easily achieved. The asymmetrical circuit model has more freedom to design different balanced circuits. The proposed balanced filter has advantages of high selectivity, high passband-order and wideband harmonic/common mode suppression.

ACKNOWLEDGMENT

This work is supported by by Jinling Institute of Technology under Grant JIT-b-201423, JIT-2016-jlxm-23 and Natural Science Foundation of Jiangsu Province (BK20130096).

REFERENCES

1. Eisenstant, W. R., B. Stengel, and B. M. Thompson, *Microwave Differential Circuit Design Using Mixed-mode S-parameters*, Artech House, Boston, MA, USA, 2006.
2. Feng, W. J., W. Q. Che, and Q. Xue, "The proper balance: Overview of microstrip wideband balanced circuits with wideband common mode suppression," *IEEE Microw. Magazine*, Vol. 16, No. 5, 55–68, Jun. 2015.
3. Wu, C.-H., C.-H. Wang, and C. H. Chen, "Balanced coupled-resonator bandpass filters using multi-section resonators for common-mode suppression and stopband extension," *IEEE Trans. Microw. Theory Techn.*, Vol. 55, No. 8, 1756–1763, Aug. 2007.
4. Shi, J. and Q. Xue, "Dual-band and wide-stopband single-band balanced bandpass filters with high selectivity and common-mode suppression," *IEEE Trans. Microw. Theory Techn.*, Vol. 58, No. 8, 2204–2212, Aug. 2010.
5. Lim, T. B. and L. Zhu, "A differential-mode wideband bandpass filter on microstrip line for UWB application," *IEEE Microw. Wireless Compon. Lett.*, Vol. 19, No. 10, 632–634, Oct. 2009.
6. Wu, X. and Q. X. Chu, "Compact differential ultra-wideband bandpass filter with common-mode suppression," *IEEE Microw. Wireless Compon. Lett.*, Vol. 22, No. 9, 456–458, Sep. 2012.
7. Abbosh, A. M., "Ultrawideband balanced bandpass filter," *IEEE Microw. Wireless Compon. Lett.*, Vol. 21, No. 9, 480–482, Sep. 2011.
8. Lu, Y.-J., S.-Y. Chen, and P. Hsu, "A differential-mode wideband bandpass filter with enhanced common-mode suppression using slotline resonator," *IEEE Microw. Wireless Compon. Lett.*, Vol. 22, No. 10, 503–505, Oct. 2012.
9. Lee, C.-H., C. I. G. Hsu, and C.-J. Chen, "Band-notched balanced UWB BPF with stepped-impedance slotline multi-mode resonator," *IEEE Microw. Wireless Compon. Lett.*, Vol. 22, No. 4, 182–184, Apr. 2012.
10. Shi, J., J. X. Chen, Q. Y. Lu, Y. Peng, and Z. Bao, "Compact low-loss wideband differential bandpass filter with high common-mode suppression," *IEEE Microw. Wireless Compon. Lett.*, Vol. 23, No. 9, 480–482, Sep. 2013.
11. Wang, X.-H., Q. Xue, and W.-W. Choi, "A novel ultra-wideband differential filter based on double-sided parallel-strip line," *IEEE Microw. Wireless Compon. Lett.*, Vol. 20, No. 8, 471–473, Aug. 2010.
12. Feng, W. J., W. Q. Che, T. F. Eibert, and Q Xue, "Compact wideband differential bandpass filter based on the double-sided parallel-strip line and transversal signal-interaction concepts," *IET Microw. Antennas Propag.*, Vol. 6, No. 2, 186–195, Apr. 2012.
13. Feng, W. J., W. Q. Che, Y. L. Ma, and Q Xue, "Compact wideband differential bandpass filter using half-wavelength ring resonator," *IEEE Microw. Wireless Compon. Lett.*, Vol. 23, No. 2, 81–83, Feb. 2013.
14. Feng, W. J. and W. Q. Che, "Novel wideband differential bandpass filters based on T-shaped structure," *IEEE Trans. Microw. Theory Techn.*, Vol. 60, No. 6, 1560–1568, Jun. 2012.
15. Martínez, J. J. S. and E. M. Segura, "Analytical design of wire-bonded multiconductor transmission-line-based ultra-wideband differential bandpass filters," *IEEE Trans. Microw. Theory Techn.*, Vol. 62, No. 10, 2308–2315, Oct. 2014.
16. Matthaei, G., L. Young, and E. M. T. Jones, *Microwave Filters, Impedance Matching Networks and Coupling Structures*, Section 5, 222–224, Artech House Inc., Norwood, MA, 1985.